

---

# Polaron-Induced Conformation Change in Single Polypyrrole Chain: An Intrinsic Actuation Mechanism

---

XI LIN,<sup>1</sup> JU LI,<sup>2</sup> ELISABETH SMELA,<sup>3</sup> SIDNEY YIP<sup>1</sup>

<sup>1</sup>Department of Nuclear Engineering and Department of Materials Science and Engineering, Massachusetts Institute of Technology, Cambridge, Massachusetts 02139

<sup>2</sup>Department of Materials Science and Engineering, Ohio State University, Columbus, Ohio 43210

<sup>3</sup>Department of Mechanical Engineering, University of Maryland, College Park, Maryland 20742

Received 29 September 2004; accepted 18 October 2004

Published online 14 January 2005 in Wiley InterScience (www.interscience.wiley.com).

DOI 10.1002/qua.20433

---

**ABSTRACT:** Ab initio calculations show that a neutral polypyrrole chain in the ground state assumes a helical shape resulting from a novel bending mechanism, while upon oxidation the chain becomes planar within the polarons, an effect due to enhanced inter-ring  $\pi$  bonding. This polaron-induced conformation change leads to an intrinsic potential for inducing macroscopic strains in the single chain, with implications for further theoretical studies and experiments. © 2005 Wiley Periodicals, Inc. Int J Quantum Chem 102: 980–985, 2005

**Key words:** polypyrrole; conjugated polymer; polaron; conformation; actuation mechanism; helix

---

**H**elical structures have recently attracted much interest in the field of  $\pi$ -conjugated polymers [1–5]. Helices may arise for a variety of reasons, such as hydrogen bonding [4], steric interactions between sidechains [5], twisting with a polymeric dopant, or polymerization in a chiral medium [2, 3].

Correspondence to: S. Yip; e-mail: syip@mit.edu

Contract grant sponsors: Honda R&D Co., Defense Advanced Research Projects Agency (DARPA)/Office of Naval Research (ONR), National Science Foundation (NSF), Lawrence Livermore National Laboratory (LLNL), Ohio State University (OSU) Transportation Research Endowment Program, and Dupont Young Professor Grant.

It was observed via small-angle neutron scattering that upon oxidation, single poly-(3-alkylthiophene) chains undergo large conformational changes from coils to rods [6]. Two questions are of interest: i) How does a single conjugated polymer chain form coils or even helices? ii) What causes the chain conformation to change in the oxidation-reduction (redox) processes? Although the theory of solitons and polarons has been successful in explaining many electronic and optical properties of conjugated polymers [7], thus far a direct connection with chain conformation has not been established. In the classical picture of polarons, in which an electron or hole couples to an optical phonon,

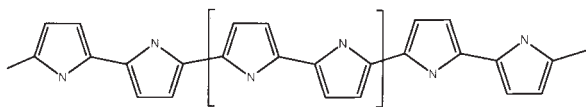


**FIGURE 1.** Chemical structure of a polypyrrole chain.

within the polaron the long bonds are shortened and short bonds lengthened, such that the total carbon backbone length is largely unchanged. Thus, it would appear that polarons would not play any significant role in processes giving rise to significant macroscopic strains. Yet this is what we find from *ab initio* calculations on single polypyrrole (Fig. 1) chains.

We investigate the intrinsic connection between polaron and actuation by presenting three closely related results. These are: i) a neutral pyrrole (P) oligomer, starting from 2P, is nonplanar due to the preference of finite dihedral angles; ii) as a unique geometrical consequence of the five-membered pyrrole ring, alternating  $+ - + -$  dihedral angles lead to helical ground-state structures, a mechanism which is entirely different from the energetically unfavorable helical defects [8] such as  $180^\circ$  rotation of alternating pyrrole units; iii) by coupling to the dihedral angles to favor a locally planar orientation in its quinoid core, a polaron is able to induce a macroscopic shape change in the oligomer. Our results thus suggest a possible nanoscale single-molecule actuation mechanism driven by redox that is intrinsic to the pyrrole chain, in the sense that the counter ions and interchain interactions are not involved. A similar approach was adopted in the early discussions of charge transport [7] in these systems.

In view of the intensive discussions of planarity [9–13] versus nonplanarity [4–16] in both the experimental and computational literature for simple  $\pi$ -conjugated oligomers without bulky side groups (excluding the case of polyaniline, which contains N atoms with electron lone pairs in the 1D backbone, and thus nonplanar neutral states are well documented [17]), we began with a consideration of the planarity of a pyrrole dimer, 2P, in the ground state. We used Gaussian-03 [18] at the level of second-order truncated Møller-Plesset correlation energy correction (MP2) with the basis set of 6-31++G(d,p). The potential energy surface for the neutral 2P (see Fig. 2) shows that the torsion angles of  $0^\circ$  and  $180^\circ$  between the rings are saddle-points, whereas the stable configuration has a value of  $47^\circ$  with an energetic preference of 0.09 eV over the  $0^\circ$

configuration. As a check of the MP2 results, we performed more accurate calculations at the torsion angles of  $0^\circ$  and  $47^\circ$  using fourth-order-truncated Møller-Plesset correlation energy corrections (MP4-STDQ), quadratic configuration interaction corrections (QCISDT), and coupled cluster with single and double substitutions (CCSD). We obtained energy differences of 0.08, 0.07, and 0.07 eV which we believe are consistent with the accuracy one should ascribe to the MP2 results. Our interpretation of the  $47^\circ$  torsion angle is that it results from the competition between backbone  $\pi$ -conjugation that favors  $0^\circ$  and Peierls distortion, aromatic ring, and steric effects that favor  $90^\circ$ . The bridge C–C bond is a mixture of single and double bonds; its length of 1.45 Å at equilibrium is roughly halfway between the typical 1.54 Å C–C single and 1.33 Å double bond lengths.

The nonplanarity of the 2P systems is governed by the bonding characteristics at the bridge site. We used molecular orbital (MO) theory to analyze the behavior of the  $\pi$ -orbitals, which have distinct phase separations, or nodes in the wavefunction.

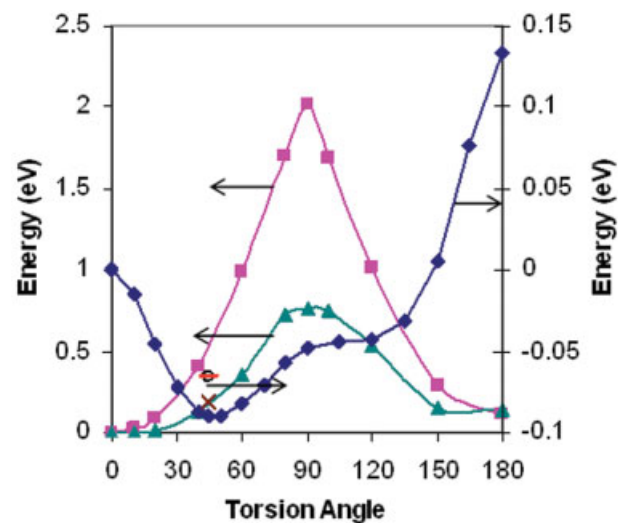


**FIGURE 2.** Potential energy surfaces of neutral (blue diamonds), singly oxidized (green triangles), and doubly oxidized (pink squares) 2P and along the inter-ring torsion direction computed by MP2. Note that the torsion angle in this figure is defined with the reference of having the two N atoms on different sides of the rings. MP4(SDTQ), QCISD(T), and CCSD results of the  $47^\circ$  ground state are marked as the brown cross, the black circle, and the red dash, respectively. All energies are computed with respect to the planar reference of  $0^\circ$  as shown. [Color figure can be viewed in the online issue, which is available at [www.interscience.wiley.com](http://www.interscience.wiley.com).]

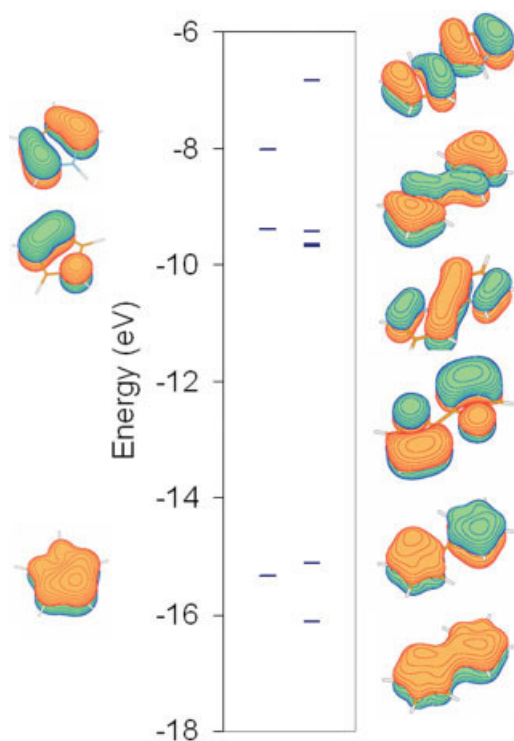


**FIGURE 3.** The complete sets of occupied  $\pi$ -orbitals of the pyrrole ring P (fully relaxed, left) and 2P (relaxed under the planar constraint, right). [Color figure can be viewed in the online issue, which is available at [www.interscience.wiley.com](http://www.interscience.wiley.com).]

The complete set of six occupied  $\pi$ -orbitals of 2P along the carbon backbone (right column of Fig. 3) consists of three bonding and three antibonding orbitals, without and with nodes at the bridge, respectively. It follows that for 2P in the neutral state, in which all six  $\pi$ -orbitals are occupied, complete cancellation of bonding and antibonding among the orbitals leaves no net  $\pi$  bond at the bridge. There is then no reason for the stable configuration to be planar. By the same token, when one or more electrons are removed it is possible for local planarity to be maintained.

The highest occupied molecular orbital (HOMO) (the top orbital of the right column in Fig. 3) has three nodes along the carbon backbone, the middle node being at the bridge site, indicating antibonding characteristics. When one or two electrons are removed from the HOMO, then cancellation is incomplete such that the net bonding characteristic of all the lower orbitals gives a planar conformation. This situation does not change upon removing three electrons, but if four electrons are removed,

the overall  $\pi$  bond at the bridge site for the system again disappears. On this basis one expects  $2P^+$ ,  $2P^{2+}$ , and  $2P^{3+}$  to be planar, but  $2P$  and  $2P^{4+}$  to be nonplanar. Indeed, these are the results obtained in our MP2 calculations. (We determined these local minimum states, but their lifetimes were not calculated.) The change between planar and nonplanar conformations is significant in conjugated polymer actuators because the resulting chain movements are thought to play a role in hysteresis [19] and conformational relaxation [20], and we now have a theoretical basis for this behavior.

Given that the equilibrium torsion angle between the two rings in neutral 2P is nonzero, there are two possible torsional conformations for 3P when a third pyrrole ring is added. In MP2 calculations, the conformation with one  $+44^\circ$  torsion and one  $-44^\circ$  torsion is more stable by 0.01 eV than that with two  $+44^\circ$  torsions. This is a full 0.16 eV lower in energy than the planar conformation with two  $0^\circ$  angles. Similarly, for 4P the conformation with  $+--+$  ( $44^\circ, -40^\circ, 44^\circ$ ) is lower in energy by 0.01 eV than  $++-$  ( $45^\circ, 42^\circ, -44^\circ$ ) and 0.01 eV lower than  $+++$  ( $40^\circ, 38^\circ, 40^\circ$ ). These results indicate that the torsional angles are only weakly coupled to each other, which in turn implies an energetic preference for nonplanarity in the longer neutral pyrrole chains. Note that the small deviations in the torsion angle values reflect minor boundary effects at the ends of the 1D polymer chain.

MP2 calculations become impractical for systems larger than 4P, so we turned to less accurate Hartree-Fock (HF) and Density Functional Theory (DFT) calculations in order to study longer oligomers. Starting with 2P and using HF/3-21G, DFT/B3LYP/3-21G, and HF/6-31++G(d,p), we obtained torsional angles of  $24^\circ$ ,  $18^\circ$ , and  $33^\circ$ , respectively, appreciably smaller than that predicted by the MP2 methods.

In using DFT we encountered difficulties in describing the localization of polarons and polarizability [13, 21–23] because the density functionals used are incapable of treating enhanced exchange effects among  $\pi$  electrons [24], compared to averaged exchange effects of all (both  $\sigma$  and  $\pi$ ) electrons [25]. Thus, we will focus on the HF results from here on. One potential alternative solution is to use time-dependent current density functional theory, where nonlocality of the exchange-correlation functional may be reflected [26].

Since many combinations of  $+$  and  $-$  are possible in making up a torsional sequence, we considered two extremes: uniform ( $+++...$ ) and alternating

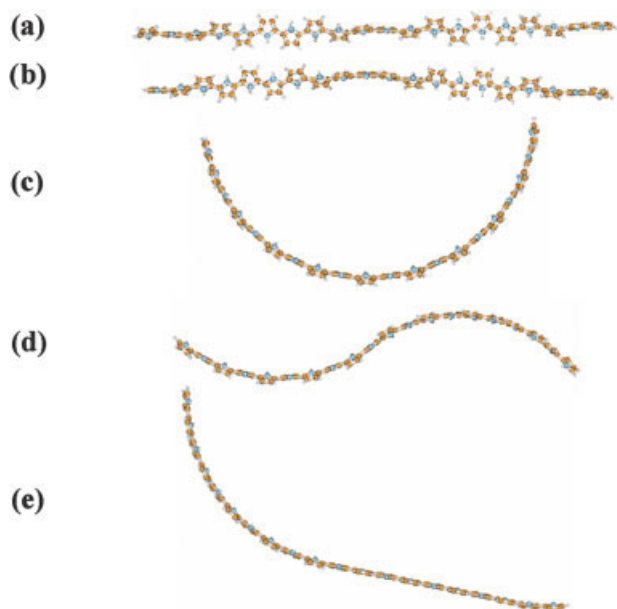


**FIGURE 4.** a: Twisted (. . . + + + . . .); b: dual-twisted (. . . + + + - - - . . .); c: bent (. . . + - + - + - . . .); d: dual-bent (. . . + - + + - + . . .) secondary structures of a neutral pyrrole oligomer 20P; and e: its bipolaron state computed by HF/3-21G. Note that HF/3-21G gives a torsion angle of  $24^\circ$  at neutral, smaller than the  $45^\circ$  predicted by more accurate MP2 methods. Identical scale is chosen for all structures for comparison. In addition, partially oxidized state, showing planar segments, can be seen in (e). [Color figure can be viewed in the online issue, which is available at [www.interscience.wiley.com](http://www.interscience.wiley.com).]

(+ - + - . . .) sequences. For the former case we find a twisted structure for a 20P chain, as shown in Figure 4a,b. Because HF is less accurate than MP2, we used the latter value for the torsion angle ( $45^\circ$ ) to estimate the diameter and pitch for the 20P helical structure, obtaining 0.5 nm and 2 nm, respectively.

The latter case of alternating sequence + - + - is actually found to be the ground state of  $nP$ , according to MP2 calculations up to 4P and HF calculations out to 30P. Because the five-membered pyrrole rings are interconnected through  $\alpha$ -carbons, the ground-state conformation with an alternating sequence can take on a variety of structures, all with an overall bent characteristic. Two such structures, the bent and dual-bent, or S-shape, of a 20P chain determined by HF/3-21G are shown in Figure 4c,d. The bent conformation is rather novel; it occurs in conjugated polymers of five-member rings, such as polypyrrole or polythiophene, but not in six-member rings connected at the para-

positions, such as poly(p-phenylene). This is because the two torsion axes on the same pyrrole unit are not parallel to each other. Thus, one axis rotating by  $\theta$  while the other axis rotating by  $-\theta$  does not result in complete cancellation.

Previously, a bending mode was expected only in the presence of defects, such as counterions and/or having all the nitrogen atoms of adjacent pyrrole rings located on the same side of the chain [10, 27]. In contrast, the present results show that the bent structure is an inherent property of the ground state of neutral polypyrrole. A bent conformation can manifest a variety of secondary structures (although we would not expect to see these at room temperature since the energy difference between ++ and +- is lower than  $k_B T$ ). It can be proven that with alternating but equal torsion angles, the atoms on every other pyrrole ring are located on one plane [24]. Loops and even closed rings are theoretically possible, moieties which are crucial to interlocked, intertwined, and Möbius structures [8, 28, 29]. A computed ring of 22P based on HF/3-21G with fixed torsional angles of  $45^\circ$  is shown in Figure 5 (left). The estimated diameter of the ring is 2.5 nm. For a chain of more than 22 units, an alternating torsion angle sequence invariably leads to the helical structure (see, for example, the HF/3-21G helix of 30P in Fig. 5, right). The corresponding diameter and pitch are estimated to be 2.2 nm and 0.6 nm, respectively.

As discussed in the molecular orbital analysis of oxidized 2P, removing an electron effectively increases the strength of the bridge bond between the two pyrrole rings. In all the  $nP$  calculations, the HOMOs are found to have the same pattern as the



**FIGURE 5.** Ring 22P ( $44^\circ$  torsion angles, left) and helical 30P (fixed  $45^\circ$  torsion angles, right) secondary structures of pyrrole oligomers computed by HF/3-21G. [Color figure can be viewed in the online issue, which is available at [www.interscience.wiley.com](http://www.interscience.wiley.com).]

one shown in Figure 3. One therefore expects that upon oxidation to a state corresponding to one charge per three pyrrole rings (30% oxidized), which is a typical experimental maximum doping level, twisted and bent secondary structures should disappear and the chain become planar in the ground state. Local planarity was demonstrated by an HF/3-21G computation on  $20P^{2+}$ , as shown in Figure 4e. We note the associated local charges and local bond-length smoothing which have been mentioned in previous studies [13, 21]. In Figure 4 one can clearly see the straightening of the charged chain segment consisting of eight pyrrole units.

Using the change in end-to-end distance for the 20P chain we find significant strains from the charge-induced conformational change of the calculated oligomer. We estimate the induced strains in unbending a 20P upon oxidation to  $20P^{2+}$  to be 31%. One might also expect large stiffness changes in the oxidized chains relative to the neutral ones. From the results given in Figure 2, we estimate a local torsion modulus (curvature of energy-strain variation) for the 30% oxidized state to be 10 MPa. The stiffness increases with oxidation level.

By investigating the conformational characteristics of a particular conjugated polymer, polypyrrole, we find polarons may have a more significant role in the molecular origin of macroscopic strains than previously recognized. A neutral pyrrole oligomer, starting from the pyrrole dimer, is nonplanar; as a result, the secondary structures of a neutral chain take on twisted and bent/helical shapes in the ground state. Unlike hydrogen bonding in proteins, the helical structures are generated through the torsions of  $\pi$ -conjugated five-membered pyrrole units. Furthermore, polarons favor a zero dihedral angle locally; thus, macroscopic shape changes can manifest in the oligomer upon oxidation, leading to large strain and stiffness changes. This suggests a possible single-chain actuation mechanism driven by oxidation and reduction processes. The mechanism is intrinsic since interchain interactions or counterions are not required; it offers a physical interpretation of the large conformational changes observed in doped single poly-3-butylthiophene chain by small-angle neutron scattering [6]. (Conjugated polymers are widely studied for their actuation properties, but in the devices demonstrated to date the actuation has been primarily due to ion and solvent insertion [30, 31].) Because it does not involve ion intercalation, the actuation process could be extremely fast; namely, this mechanism may add to our repertoire of molecular machines,

such as molecular elevator [6] and single carbon nanotube [32]. Strain measurements in single nanotubes using a conducting AFM tip suggest an approach for experiments on helical oligomers. From the theoretical point of view, the existence of secondary structures presents an opportunity to expand on the traditional soliton/polaron theory [17]. Polymers of practical interest such as polypyrroles are ground state nondegenerate in terms of bond alternations, but ground state degenerate in terms of torsional motions. Moreover, the torsions are coupled to the electronic structure [17]. The theoretical formalisms for describing conducting polymers need to be modified to include these additional effects.

#### ACKNOWLEDGMENTS

We are grateful for discussions with Patrick Anquetil, John Madden, Ian Hunter, and Kazu Kawagawa.

---

#### References

- Green, M. M.; Peterson, N. C.; Takahiro, S.; Teramoto, A.; Cook, R.; Lifson, S. *Science* 1995, 268, 1860–1866.
- Akagi, K.; Piao, G.; Kaneko, S.; Sakamaki, K.; Shirakawa, H.; Kyotani, M. *Science* 1998, 282, 1683–1686.
- Yashima, E.; Maeda, K.; Okamoto, Y. *Nature* 1999, 399, 449–451.
- Cornelissen, J. J. L. M.; Donners, J. J. J. M.; de Gelder, R.; Graswinckel, W. S.; Metselaar, G. A.; Rowan, A. E.; Sommerdijk, N. A. J. M.; Nolte, R. J. M. *Science* 2001, 293, 676–680.
- Shinohara, K.-I.; Yasuda, S.; Kato, G.; Fujita, M.; Shigekawa, H. *J Am Chem Soc* 2001, 123, 3619–3620.
- Aime, J. P.; Bargain, F.; Schott, M.; Eckhardt, H.; Miller, G. G.; Elsenbaumer, R. L. *Phys Rev Lett* 1989, 62, 55–58.
- Heeger, A. J.; Kivelson, S.; Schrieffer, J. R.; Su, W.-P. *Rev Mod Phys* 1988, 60, 781–851.
- Mena-Osteritz, E.; Meyer, A.; Langeveld-Voss, B. M. W.; Janssen, R. A. J.; Meijer, E. W.; Bauerle, P. *Angewandte Chem Int Ed* 2000, 39, 2680–2684.
- Street, G. B.; Lindsey, S. E.; Nazzal, A. I.; Wynne, K. J. *Mol Crystals Liq Crystals* 1985, 118, 137–148.
- Saunders, B. R.; Fleming, R. J.; Murray, K. *Chem Mater* 1995, 7, 1082–1094.
- Brédas, J. L.; Silbey, R.; Boudreaux, D. S.; Chance, R. R. *J Am Chem Soc* 1983, 105, 6555–6559.
- Brédas, J. L.; Thémans, B.; André, J. M. *Phys Rev B* 1983, 27, 7827–7830.
- Geskin, V. M.; Dkhissi, A.; Brédas, J. L. *Int J Quantum Chem* 2002, 91, 350–354.
- Kofranek, M.; Kovar, T.; Karpfen, A.; Lischka, H. *J Chem Phys* 1992, 96, 4464–4473.

15. Colle, R.; Curioni, A. *J Phys Chem A* 2000, 104, 8546–8550.
16. Yurtsever, M.; Yurtsever, E. *Synthetic Metals* 1999, 98, 221–227.
17. MacKenzie, R.; Ginder, J. M.; Epstein, A. J. *Phys Rev B* 1991, 44, 2362–2365.
18. Frisch, M. J.; Trucks, G. W.; Schlegel, H. B.; Scuseria, G. E.; Robb, M. A.; Cheeseman, J. R.; Zakrzewski, V. G.; Montgomery Jr, J. A.; Stratmann, R. E.; Burant, C.; Dapprich, S.; Millam, J. M.; Daniels, J. D.; Kudin, K. N.; Strain, M. C.; Farkas, O.; Tomasi, J.; Barone, V.; Cossi, M.; Cammi, R.; Mennucci, B.; Pomelli, C.; Adamo, C.; Clifford, S.; Ochterski, J.; Petersson, G. A.; Ayala, P. Y.; Cui, Q.; Morokuma, K.; Rega, N.; Salvador, P.; Dannenberg, J. J.; Malick, D. K.; Rabuck, A. D.; Raghavachari, K.; Foresman, J. B.; Cioslowski, J.; Ortiz, J. V.; Baboul, A. G.; Stefanov, B. B.; Liu, G.; Liashenko, A.; Piskorz, P.; Komaromi, I.; Gomperts, R.; Martin, R. L.; Fox, D. J.; Keith, T.; Al-Laham, M. A.; Peng, C. Y.; Nanayakkara, A.; Challacombe, M.; Gill, P. M. W.; Johnson, B.; Chen, W.; Wong, M. W.; Andres, J. L.; Gonzalez, C.; Head-Gordon, M.; Replogle, E. S.; Pople, J. A. *Gaussian, Inc.: Pittsburgh PA*, 2003.
19. Heinze, J. *Synthetic Metals* 1991, 43, 2805–2823.
20. Otero, T. F.; Grande, H. J. *Colloid Surf A-Physicochem Eng Asp* 1998, 134, 85–94.
21. Zuppiroli, L.; Bieber, A.; Michoud, D.; Galli, G.; Gygi, F.; Bussac, M. N.; André, J. J. *Chem Phys Lett* 2003, 374, 7–12.
22. Rubio-Pons, O.; Luo, Y. *J Chem Phys* 2004, 121, 157–161.
23. Jacquemin, D.; André, J.-M.; Perpete, E. A. *J Chem Phys* 2004, 121, 4389–4396.
24. Lin, X.; Li, J.; Yip, S. (to be submitted 2004).
25. Slater, J. C. *Phys Rev* 1951, 81, 385–390.
26. van Faassen, M.; de Boeij, P. L.; van Leeuwen, R.; Berger, J. A.; Srijders, J. G. *Phys Rev Lett* 2002, 88, 186401.
27. Tamm, T.; Tamm, J.; Karelson, M. *Int J Quantum Chem* 2002, 88, 296–301.
28. Ajami, D.; Oeckler, O.; Simon, A.; Herges, R. *Nature* 2003, 426, 819–821.
29. Amabilino, D. B.; Stoddart, J. F. *Chem Rev* 1995, 95, 2725–2828.
30. Baughman, R. H.; Shacklette, L. W.; Elsenbaumer, R. L.; Plichta, E. J.; Becht, C. In *Molecular Electronics*; Lazarev, P. I., Ed.; Kluwer: Dordrecht, Netherlands, 1991, p 267.
31. Otero, T. F.; Grande, H.-J. In *Handbook of Conducting Polymers*; Skotheim, T. A.; Elsenbaumer, R. L.; Reynolds, J. R., Eds.; Marcel Dekker: New York, 1998, p 1015–1028.
32. Roth, S.; Baughman, R. H. *Curr Appl Phys* 2002, 2, 311–314.